Postprint of: Ben Tahar A., Sadowska K., Biernat J., Paluszkiewicz E., Cinquin P., Martin D., Zebda A.: High catalytic performance of laccase wired to naphthylated multiwall carbon nanotubes BIOSENSORS & BIOELECTRONICS Vol. 151, (2020), pp.1-8 DOI: 10.1016/j.bios.2019.111961

High catalytic performance of *laccase* wired to naphthylated multiwall carbon nanotubes

A B S T R A C T

The direct electrical connection of laccase on the electrode surface is a key feature in the design of efficient and stable biocathodes. However, laccase can perform a direct electron transfer only when it is in the preferred orientation toward the electrode. Here we report the investigation of the orientation of laccase from white rot fungus on multi-walled carbon nanotube surface modified with a naphthalene group. Naphthylated multi wall carbon nanotubes were synthesized and the kinetics of laccase from white rot fungus adsorption and its direct electro-catalytic activity toward oxygen reduction was investigated by QCM and electrochemical techniques. Compared to pristine multi-walled carbon nanotubes laccase shows a high affinity to be adsorbed onto the surface of naphthylated carbon nanotubes at a very fast rate. The subsequent wiring to the naphthylated multi- walled carbon nanotubes is accompanied by a reorientation and arrangement of adsorbed laccase to create a composite biocathode that exhibits a high-performance for oxygen reduction by direct electron transfer with maximum current densities of 3 mA cm^{-2}.

1. Introduction

The enzyme laccase was described for the first time by Yoshida in 1883 (Yoshida, 1883), and since then it is used widely in science and industry. Laccases belong to multicopper oxidases that catalyze the oxidation of a wide variety of organic substrates followed by dioxygen reduction to water according to four-electron mechanism (Le Goff et al., 2015). Laccase has four copper atoms in the active centre of the enzyme and they are known as copper type 1 (T1), copper type 2 (T2) and two copper type 3 (T3) centers (Bertrand et al., 2002; Solomon et al., 2014). It is widely accepted that centre T1, called "copper blue", takes electrons from the substrate which is oxidized (or it oxidizes), and transfers them to the T2/T3 cluster (TNC Trinuclear Cluster) responsible for the four-proton along with four-electron reduction of O_2 into water (Ber-trand et al., 2002; Solomon et al., 2014). The T1 is connected to the centre T2/T3 by a triad of amino acids Histidine-Cysteine-Histidine (His-Cys-His) which is common to all metalloenzymes called laccases.

The capability of laccase to catalyze the reduction of oxygen to water makes it an ideal biocathode catalyst for application in biofuel cells (Le Goff et al., 2015; Bertrand et al., 2002).

The electrical connection of laccase and its orientation on the elec-trode surface are key features in the design of efficient and stable bio-cathodes. However, as a vast majority of the oxidoreductases, laccases can perform a direct electron transfer only when they are in the pref-erable orientation toward the electrode (Blanford et al., 2007a). In the case of laccase, the direct electron transfer is possible when its active center T1 is close to the electrode surface, which requires a control of laccase molecule orientation on the electrode surface (Arrocha et al., 2014; Blanford et al., 2007b). However, some authors discussed, whether direct electron transfer between laccase and the electrode can be achieved *via* the T2/T3 center. In this case the T1 center will be not participating in the electrocatalytic activity of laccase on the electrode surface (Shleev et al., 2005; Pita et al., 2006).

As the enzyme orientation is one of the key factors influencing the electrode performance, different approaches were proposed to assure its best connection with the electrode. Armstrong et al. smartly conducted an alternative to covalent immobilization of enzyme. They aligned and immobilized laccase on graphitic surfaces, which were previously covalently modified with anthracene or anthraquinone residues (Blan-ford et al., 2008). In this approach, the laccase adsorption on electrode surface was governed by the hydrophobic-hydrophobic interactions between anthracene (or anthraquinone) residue and the hydrophobic pocket of laccase, where the T1 center is located. This approach was used by many authors to control the orientation of laccase on the surface of different materials including carbon nanotubes (CNTs) widely used for the construction of enzymatic electrodes (Sadowska et al., 2008; Sadowska, Roberts, Wiser, Biernat, Jabłonowska, Bilewicz; Kariuki and McDermott, 1999; Bahr et al., 2001). In our previous papers systematic studies of catalytic activity of biocathode components, its constitution and texture on electrode behavior was reported (Rebelo et al., 2016; Osswald et al., 2007). It was found that the most effective charge con-ducting substituents directly attached to SWCNTs are phenyl, naphthyl, anthryl, terphenyl and anthraquinyl residues.

The enzyme laccase was described for the first time by Yoshida in 1883 (Yoshida, 1883), and since then it is used widely in science and industry. Laccases belongs to a class of multicopper oxidases that cata-lyze the oxidation of a wide variety of organic substrates followed by dioxygen reduction to water according to four-electron mechanism (Le Goff et al., 2015). Laccase has four copper atoms in the active centre of the enzyme and they are known as copper type 1 (T1), copper type 2 (T2) and two copper type 3 (T3) centers (Bertrand et al., 2002; Solomon et al., 2014). It is widely accepted that centre T1, called "copper blue", takes electrons from the substrate which is oxidized (or it oxidizes), and transfers them to the T2/T3 cluster (TNC Trinuclear Cluster) responsible for the four-proton along with four-electron reduction of O2 into water (Bertrand et al., 2002; Solomon et al., 2014). The T1 is connected to the centre T2/T3 by a triad of amino acids Histidine-Cysteine-Histidine (His-Cys-His) which is common to all metalloenzymes called laccases. The capability of laccase to catalyze the reduction of oxygen to water makes it an ideal biocathode catalyst for application in biofuel cells (Le Goff et al., 2015; Bertrand et al., 2002).

The electrical connection of laccase and its orientation on the elec-trode surface are key features in the design of efficient and stable bio-cathodes. However, similar to a vast majority of the oxidoreductases, laccase can perform a direct electron transfer only when it is in the preferred orientation toward the electrode (Blanford et al., 2007a). This is when its active center T1 is close to the electrode surface, which re-quires control of the orientation of the laccase molecule on the electrode surface (Arrocha et al., 2014; Blanford et al., 2007b). However, some authors have discussed whether direct electron transfer between laccase and the electrode can be achieved *via* the T2/T3 center. In that case the T1 center will not participate in the electrocatalytic activity of laccase on the electrode surface (Shleev et al., 2005; Pita et al., 2006).

A Since the enzyme orientation is one of the key factors influencing the electrode performance, different approaches have been proposed to assure its best connection with the electrode. Armstrong et al. reported an innovative alternative to covalent immobilization of the enzyme. They aligned and immobilized laccase on graphitic surfaces, which were previously covalently modified with anthracene or anthraquinone residues (Blanford et al., 2008). In that approach, the laccase adsorption on the electrode surface was governed by the hydrophobic-hydrophobic interactions between the anthracene (or anthraquinone) residue and the hydrophobic pocket of laccase, which is the location of the T1 center. That approach was used by many authors to control the orientation of laccase on the surface of different materials widely used for the con-struction of enzymatic electrodes, including carbon nanotubes (CNTs) (Sadowska et al., 2008; Sadowska, Roberts, Wiser, Biernat, Jabło-nowska, Bilewicz; Kariuki and McDermott, 1999; Bahr et al., 2001). Indeed, we have previously reported systematic studies of the catalytic activity of biocathode components, including the constitution and texture, on electrode behavior (Rebelo et al., 2016; Osswald et al., 2007). We found that the most effective charge conducting substituents directly attached to SWCNTs are phenyl, naphthyl, anthryl, terphenyl and anthraquinyl residues. In many respects, the described carbonaceous materials meet the properties anticipated for bioelectrodes applicable for biofuel cells (BFCs). There is dependence of the biocathode behavior on the com-ponents of cathodic compartment and, in particular, on the materials applied to assist charge exchange. Since the CNTs with aromatic residues are extremely efficient in performing the role of insoluble molecular wires, the power and current densities are very high. The last parameters presumably depend on the best fit of the aromatic substituent di-mensions (number and length of aromatic branches) attached to CNTs and the size of the hydrophobic hole of the enzyme active center. It is also known that these particular parameters depend also on the kind of carbon nanotubes and electrode arrangement.

Here we report our investigations of the direct electron transfer between *laccase* and naphthylated multi wall carbon nanotubes (MWCNTs- NA). Physical characterization of naphthalene modified MWCNTs shows a high level of functionalization whereas electrochemical studies demonstrated that *laccase* modified MWCNTs-NA exhibit a high elec-trocatalytic current density toward oxygen reduction. Moreover, we combinedQCM-D measurements with electrochemistry to investigate the relationship between the kinetic of *laccase* adsorption and its elec-trical connection to MWCNTs-NA.

2. Material and methods

Laccase Y120 from white rot fungus (Trametes sp., EC 1.10.3.2, 10 U mg 1), were kindly donated by Amano Enzyme company (Japan), NaCl, Na2HPO4 (>99%), NaH2PO4 (>99%), acetic acid 99.8%), Tween 80 solution, chitosan (medium molecular weight) were purchased from Sigma Aldrich (Saint Quentin Fallavier, France). N,N- Dimethylformamide, 1,2-dichlorobenzene, acetonitrile, 2-naphthyl-amine were delivered by Sigma Aldrich-Merck (Darmstadt, Germany). All aqueous solutions were prepared using ultrapure water with a resistivity not less than 18.2 MΩ cm at 25°C (Purelab Prima, D´ecines- Charpieu, France). A multi-walled carbon nanotubes (MWCNTs) (>95% purity, pristine MWCNTs – outer diameter <8 nm, length 10–30 nm, purity >95%) from CheapTubes, Brattleboro, USA, were used as received.

2.1. *Chemical preparation of naphthylated-MWCNT (MWCNT-NA)*

Pristine multiwalled carbon nanotubes (MWCNT 900 mg 75.1 mmol) were suspended in a solution of 2-naphthylamine (2.86 g, 20 mmol) in a mixture of 1,2-dichlorobenzene (20 mL) and acetonitrile (20 mL) and the suspension was sonicated for 20 min. This procedure causes deglomeration of nanotubes providing naphthylamine much better access to the carbonaceous surface. The mixture was than cooled to -5°C , and *i*-amyl nitrite (2.7 ml, 20.1 mmol) was added in one portion. The mixture was sonicated for 5 min at low temperature and then under permanent sonication the mixture was heated and maintained at 65 °C for 1 h and then at 70 °C for 5 h. After cooling the solid material was separated by centrifugation and the supernatant was decanted. The sediment was suspended in DMF, sonicated and centrifuged. The sedi-ment was suspended in toluene as this solvent proved to be more effective in the final stage of nanotubes purification, which can be explained by the competitive π - π interaction of toluene with impurities. The yield of pure material equals ~1 g.

2.2. *Bio-electrodes preparation*

The MWCNT-NA based ink was prepared by the addition of 2 mL of water containing 0.375% of Tween 80 to 5 mg of MWCNT-NA and sonicating for 30 min. The presence of Tween 80 in the water suspension aimed to improve the homogeneity of the MWCNTs-NA ink. Finally, 100 μL of the prepared ink was deposited onto the surface of glassy carbon (0.07 cm^2).

2.2.1. The field-emission gun scanning electron microscopy (FEG–SEM)

The structure of the bio-electrode was characterized by FEG-SEM using an ULTRA 55 FESEM based on the GEMINI FESEM column (Nanotechnology Systems Division, Carl Zeiss NTS GmbH). Samples were sputter-coated with 1 nm gold-palladium bilayer using a precision etching coating system (PSCE 682- Gatan, Inc., CA).

2.2.2. BET surface area of porous carbon

The surface area of the MWCNTs samples was determined by Bru-nauer–Emmett–Teller (BET) measurements: using a Micromeritics ASAP 2020 instrument to acquire the N2 adsorption–desorption isotherms. The samples were previously degassed at ambient temperature for 2 h. Average pore size distribution was calculated using the Barrett-Joynes- Halenda (BJH) method (Antunes et al., 2006).

2.2.3. Electrochemical measurements

A BILOGIC Instruments 650 potentiostat interfaced to a PC was used for all experiments along with a saturated calomel electrode (SCE) as reference and a platinum mesh as the counter electrode, unless other-wise stated. Cyclic voltammograms were obtained at a scan rate of 2 mV/s. The potential window used was -1.0 to 1.0 V vs SCE. All measurements were performed at ambient temperature (20+- 3°C) in PBS buffer pH 5.

2.2.4. Thermogravimetric analysis (TGA)

Thermogravimetric analysis (TGA) was performed under argon with a heating rate 5 °C/min from 40 °C to 900° C using Netzsch STA 449 F1. The STA 449 F1 has a vertical sample carrier and in order to account for buoyancy effects, a correction curve with empty crucibles was first ob-tained and then subtracted from the experimental results. To avoid heat and mass transfer limitations, approximately 30 mg of sample was used, and Al2O3 crucibles with lids were employed. The total uncertainty associated with measurement was 0.005% by weight of the sample and was included in the result.

2.2.5. Raman spectroscopy

Raman spectra were recorded using a Renishaw InVia spectroscope with an argon ion laser operating at 514.5 nm focused through a 50x objective. Collected light was dispersed through a triple monochromator and detected with a charge-coupled device. The spectra were collected in the dark, with a resolution of 2 cm^{-1} in the range of 100–3200 cm^{-1}.

2.2.6. FTIR spectroscopy

The FTIR spectra were recorded at room temperature using Perki-nElmer spectrometer (model Frontier FTIR MIR/FIR). The FTIR spectra of the samples pressed into KBr pellets with constant measure material concentration (0.5%) were collected in the wave number range 4000–400 cm^{-1} (mid IR region) using the KBr beam splitter.

2.2.7. Quartz crystal microbalance with dissipation monitoring (QCM-D)

QCM-D measurements were performed using a QCA922A analyzer (BIOLOGIC, France). A small volume (10 μL) of the MWCNTs-NA sus-pension was deposited on a gold-film-coated AT-cut quartz crystal that had a 9 MHz fundamental resonance frequency. The quartz crystal completed the base of a 1 mL chamber, to which was added the laccase in a PBS buffer pH 5.

3. Results and discussion

The naphthylated carbon nanotubes, MWCNT-NA were prepared by free-radical approach using thermal decomposition of diazonium salts prepared in situ from 2-aminonaphthalene. It has been shown, that free radicals react not only with carbon nanotubes, but also with aromatic substituents attached to the tubes in the first reaction stage (Blanford et al., 2008; Kariuki and McDermott, 1999; Bahr et al., 2001). More, traces of azo-compounds are found among the aromatic skeleton, formed by electrophilic coupling of diazonium salts. Hence, the CNTs substituents have more complicated branched architecture, as depicted in Fig. S1. However, the system of conjugated bonds in the created structures still enables effective transfer of electrons.

Raman spectroscopy was used to confirm the functionalization of MWCNTs. Raman spectra of pristine and functionalized MWCNTs are presented in Fig. 1, and they are in agreement with data reported by other groups (Sadowska, Roberts, Wiser, Biernat, Jabłonowska, Bile-wicz; Bahr et al., 2001; Rebelo et al., 2016; Osswald et al., 2007; Antunes et al., 2006). Band G, being an analogy of band observed for graphite in Raman spectrum is observed at expected frequency equal to 1584 (+-) 2 cm^{-1}. Disorder-induced Raman band (D-band) is observed near 1346 (+-) 2 cm^{-1} and its overtone G^0 at ~ 2680 (+-) 2 cm^{-1} for both analyzed samples (pristine and naphthylated). Occurrence of several RBM signals in the range of ~170–270 (+-) 2 cm^{-1} indicates the differentiation of pristine nanotubes diameters. The RBM bands observed in the low-frequency region are characteristic for single-walled carbon nano-tubes; however, they have also been reported for thin MWCNTs. The nanotubes used in the experiments are short MWCNTs, with small di-ameters (<8 nm); therefore, the obtained spectrum is consistent with the specification given by the supplier. The creation of covalent bonds should result in changes in the RBM frequency-range. Attachment of chemical moieties to the CNTs sidewalls, affects the intensity of resonant amplified low-frequency bands. The decrease of RBM intensities is attributed to the complete disintegration of nanotubes (not occurring in this study) or the reduction in resonance enhancement of selectively functionalized CNTs (Fig. 1.2). As can be seen in Fig. 1 for MWCNT-NA no RBM bands are observed, which proves the successful functionalization.

In addition to changes in RBM range, the behavior of mode D can also provide many interesting information concerning the analyzed sample. As D-band is sensitive to the disruption of hexagonal carbon network, its intensity should increase as a consequence of covalent functionalization. A medium-high D band observed for pristine nanotubes can be due to quite small aspect ratio of CNT and the residual presence of amorphous carbon (c.a. 1% as determined by TGA). However, the intensity of D band significantly increased for naphthylated sample. Moreover, the increase of intensity ratio I_D/I_G' is suggested to be a sensitive measure of functionalization, as G^0 is independent of defect concentration.

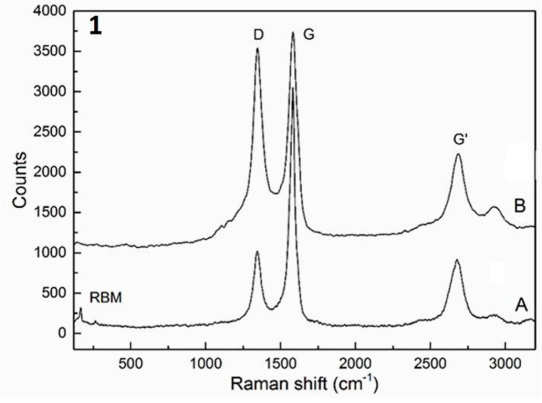

Fig. 1. (1) Raman spectra of A) pristine MWCNTs and B) MWCNTs-NA.

Therefore, the increase of D band in a relation to G and G^0 band is a confirmation of covalent CNTs functionalization. The comparison of the intensities ratio for pristine and functionalized CNTs is given in Fig. S1 (see supplementary materials). Analyzing the data presented in Table in Fig. S1, it can be concluded, that for functionalized sample the intensity of D-band increased as compared to both, G and G^0 band, being, next to the disappearance of RBM bands, an evidence of successful naphthylation. It is often observed, that the overall intensities of bands decrease after functionalization, along with bands widening. Here, the G-band intensity is similar for both samples with slight broadening observed for functionalized sample. It should be noticed, that naphthalene reveals strong Raman bands at 1382, 1464 and 1576 cm^{-1}, which are over-lapping with modes observed for carbon nanotubes. The shape and intensity of G and D band for MWCNTs-NA can be affected by the presence of attached naphthyl residues to the carbon skeleton.

The presence of naphthyl residues was also proved by FTIR spectroscopy measurements (Fig. 2.1). In the spectra of pristine MWCNTs and MWCNT-NA bands referring to C–C stretching in the carbon nano-tubes skeleton are observed at 1580 cm^{-1}. However, in the spectrum of MWCNT-NA new bands appeared which can be ascribed to stretching of C–C (at c.a. 1550 cm^{-1}) and out-of-plane C–H vibrations (in the range of 750–800 cm^{-1}) in the naphthalene units.

The purity of the nanotubes, as well as a functionalization degree can be determined by thermogravimetric analysis (TGA). Pristine and naphthylated MWCNTs were analyzed and the results are depicted in Fig. 2.2 In the case of pristine MWCNTs the total mass loss was equal to 4.91% of initial mass, which stays in agreement with specification given by a supplier, and three main steps can be distinguished. The first 0.32% mass loss is connected with water desorption. The next step observed in TG curve for pristine MWCNTs may be due to decomposition of residual groups (e.g. located at the edges of short MWCNTs) and/or some im-purities. The small (c.a. 1.3%) mass loss below 500 C informs about good quality of analyzed MWCNTs. In the highest temperature range degradation of other carbonaceous structures occurs, including the most defective carbon nanotubes. The thermogravimetric analysis of func-tionalized MWCNT-NA revealed different thermal behavior of the sample. Four degradation steps were recorded within the analyzed temperature range. First step of c.a. 1.1% mass loss is due to the solvent evaporation from the sample or removal of residual naphthyl moieties adsorbed on the MWCNTs sidewalls.

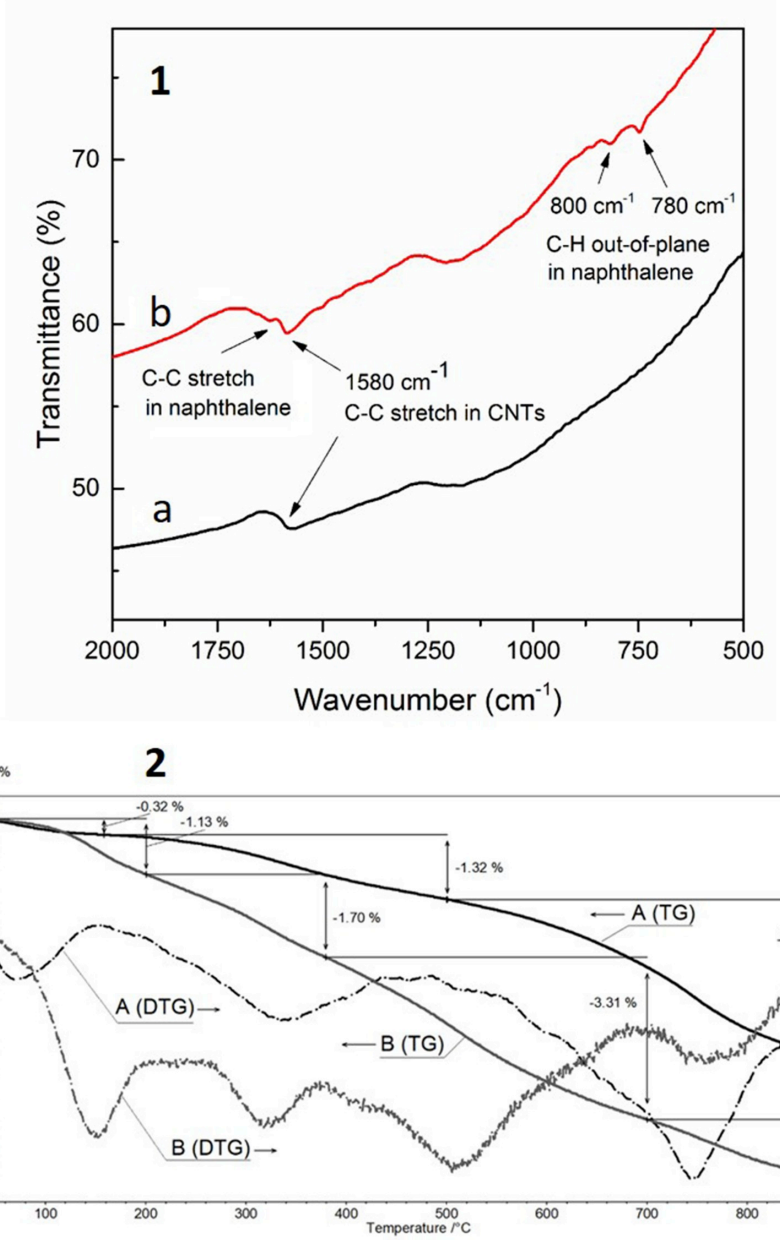

Fig. 2. (1) FTIR spectra of a) pristine MWCNTs; b) MWCNTs-NA, (B), (2) TG and DTG curves for A) pristine MWCNT and B) MWCNTs-NA.

After synthesis, the sample was thoroughly washed with different solvents, including DMF with high boiling point; therefore, the first step is finished at higher temperature as compared to pristine MWCNTs. The next step, occurring between 200- 380 °C is connected with naphthyl residues detachment, followed by further degradation of substituents up to 700 °C. Taking into account the mechanism of the reaction, described in details previously (–Zelechowska et al., 2013), branched structures composed of several naphthyl moieties are created. Such aromatic oligomers or dendritic structures (of higher molecular mass) are more thermally stable than single molecules; therefore, the observed process occurs in the higher temperature range. The cumulative mass loss ascribed to naphthyl units decomposition is comparatively high and equal to 5%. Moreover, looking at the DTG curves for both samples it can be noticed, that the degradation of carbonaceous material in MWCNT-NA sample starts at higher temper-ature and the mass loss is lower (1.2%) as compared to pristine nano-tubes (3.27%). It may be due to the removal of amorphous carbon and defective nanotubes during washing after synthesis, which was per-formed only for functionalized MWCNTs. Comparison of curves for pristine and functionalized nanotubes gives the mass of naphthyl resi-dues of about 3.31%. It can be estimated, that the mass of naphthalene units is c.a. 0.03 mg per 1 mg of MWCNT, giving $0.2 \cdot 10^{-6}$ mol of naphthyl residues in 1 mg of MWCNTs-NA.

3.1. *Kinetics of laccase adsorption*

Quartz Crystal Microbalance with Dissipation (QCM-D) is a powerful acoustic technique used commonly to measure the adsorption of small amounts of proteins [ng. cm^{-2}] onto materials surface. In addition to that, dissipation measurements that quantifies the vibrational energy an oscillator loses per cycle is used to assess the rigidity and arrangement of an adsorbed layer immediately after adsorption and to monitor conformal change of adsorbed proteins related to their rearrangements, denaturation, etc. In order to study the interactions of laccase with MWCNTs-NA, the QCM-D response of MWCNTs-NA modified gold quartz surface were studied in buffer solution (pH5) before and after the addition of 10 mM laccase in the buffer.

A typical QCM-D response is shown in Fig. 3A, where the frequency and dissipation responses are given for laccase adsorption process onto MWCNTs-NA surface. After the addition of laccase the resonance frequency decrease quickly and reaches its steady-state about 2 min after the laccase injection. This decrease corresponds to an increasing of mass on the surface of MWCNTs-NA related to the adsorption of laccase on MWCNTs. The amount of adsorbed laccase can be estimated using the equation (Sauerbrey, 1959).

$$\Delta f = \Delta m \frac{2f_0^2}{A\sqrt{\rho_q \mu_q}} \quad (1)$$

where Δm and Δf are mass change and frequency shift, respectively, A is the electrode area (0.2 cm^2), ρ_q is the density of quartz (2.65 g/cm^3), and μ_q is the shear modulus (2.95 x 10^{11} $dyncm^2$). From equation (1), we find that the mass of adsorbed laccase is 2000 (+-) 20 ng/cm^2. Taking into account that the molar weight of laccase is 65 kDA, the mass of adsorbed laccase corresponds to a molar density of 30 $pmol/cm^2$. This value is in good agreement with previous studies where blue oxidoreductase have been immobilized on AuNPs and MWCNTs (Krikstolaityte et al., 2014; Lalaoui et al., 2015). It is important to note that in our study we did not take into account the mass of coupled water sensed by QCM-D that can vary from 30% to 90% for different proteins (Bingen et al., 2008). However, we compared the density of adsorbed laccase on MWCNTs-NA with that adsorbed on pristine MWCNTs (see supplementary materials and we found out that the density of adsorbed laccase on MWCNTs-NA is two times higher than that on pristine MWCNTs that exhibits 15 $pmol/cm^2$ of adsorbed laccase. Since the specific surface area of MWCNTs-NA is similar to that of pristine MWCNTs (see supplementary materials), the high amount of adsorbed laccase on MWCNTs-NA indicates clearly that the presence of naphthyl groups on MWCNTs increased the affinity between laccase and MWCNTs surface. The examination of the dissipation response after the addition of laccase shows the presence of two regimes, the first is characterized by an increasing of the dissipation, followed by a second regime characterized by a slow decrease of the dissipation. The first regime is typical behavior of proteins adsorption on solid surface where the dissipation increase and the resonance frequency decrease. However, the second regime, where the dissipation decrease slowly, is probably due to the rearrangement of adsorbed Laccase molecules that often involves a shift of dissipation without a variation of resonance frequency. The decrease of dissipation corresponds to an improve of the rigidity of adsorbed laccase layer, which may result from an increased interaction between the adsorbed Laccase and MWCNTs-NA. To examine if there is a relationship between the electrical wiring of laccase on MWCNTs-NA surface and its adsorption kinetics, we monitored the open circuit potential (OCP) of MWCNTs-NA before and after laccase injection (Fig. 3B). First, after laccase injection, and during a few minutes, we observe a slow increase of the OCP accompanied by a slow increase of the dissipation, which indicate that the electrical connection of laccase does not happen directly after its adsorption on MWCNTs-NA. In a second period, the dissipation starts to decrease slowly, the frequency stable, and the OCP continues its slow increase to reach its maximum value of 0.58 V after 50 min. This indicate that laccase wiring to MWCNTs-NA occurs parallel with the period of rearrangement of adsorbed laccase on MWCNTS-NA. Indeed, as discussed above, frequency response indicates that laccase adsorption occurs during a short time of few minutes during which the OCP values is still low due to effect that adsorbed laccase is not yet electrically connected to the surface of the electrode These results indicate clearly that, compared to laccase adsorption on MWCNTs (see supplementary materials), electrical connection of laccase to MWCNT-NA is not fast phenomenon that occurs directly during its adsorption but results from an arrangement of adsorbed laccase molecules that favorites the orientation and wiring of laccase on MWCNTs-NA.

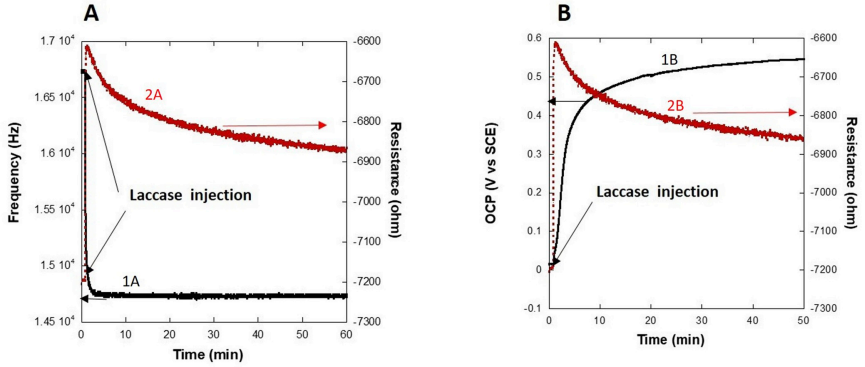

Fig. 3. (A) QCM-D response of MWCNTs-NA modified gold surface before and after laccase injection, curve 1A, Frequency response, curve 2A dissipation response. (B), evolution of the open circuit voltage (curve 1B) and the dissipation (curve 2B) of MWCNTs-NA modified gold electrode before and after laccase addition. Measurement in PBS pH5. (For interpretation of the references to colour in this figure legend, the reader is referred to the Web version of this article.)

Laccase modified MWCNT-NA GC electrodes were investigated by cyclic voltammetry in PBS buffer at pH 5.0. The cyclic voltammograms (CVs) recorded under argon and oxygen-saturated solutions are pre-sented in Fig. 4. Under oxygen conditions, the CVs exhibited a clear sigmoidal catalytic wave that corresponds to a typical behavior of an electro-catalytic reduction of oxygen that starts at 0.58 V *vs* SCE and reaches a maximum current density value of 3.3 mA cm^{-2} at 0 V. However, under nitrogen saturated condition the current density is 0.4 mA cm^{-2} and it likely corresponds only to the capacitive current. These results are 5 times higher than in the case of laccase modified pristine MWCNTs where the current density under oxygen condition is 0.6 mA/cm^2 (see supplementary materials). This value is higher than reported values of 215 $\mu A/cm^2$ on laccase adsorbed on modified SWCNTs, higher than the current density of 239 $\mu A/cm^2$ on SWCNTs-anthracene (–Zelechowska et al., 2013).

Moreover, the performances of our bioelectrode in term of current density is higher than currents density of 2.4 mA cm^{-2} obtained with laccase adsorbed on and MWCNTs-adamantane (Lalaoui et al., 2016) and also higher than reported in our previous works on laccase adsorbed on SWCNTs-NA [241 $\mu A/cm^2$] (Stolarczyk et al., 2012). The MWCNTs are considered to be all metallic, hence more uniform as compared to SWCNTs. The last are mostly used in combinations of metallic and semi-conductive in random ratios, because of the difficulty to properly separate these two forms (Grobert, 2007). However, the differences in the behavior of SW- and MWCNTs for bioelectrode modification are little understood so far (Sajjadi et al., 2011). We believe that these performances are due to the high wiring affinity between this *laccase* and MWCNTs-NA, high degree of functionalization of MWCNTs by naphthalene molecules and higher surface available for the enzyme as compared to SWCNTs, which more preferably form bundles.

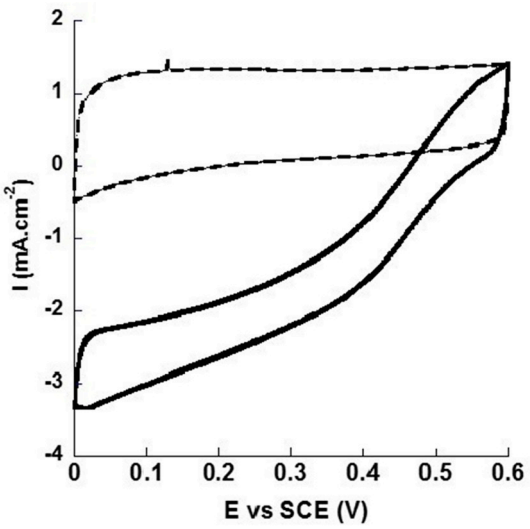

Fig. 4. Rotating disk cyclic voltammograms of catalytic dioxygen reduction at *laccase* modified MWCNTs-NA at ω ¼ 2000 rpm and v ¼ 2 mV/s under nitrogen saturated conditions (dashed line) and oxygen saturated conditions. Measure-ment carried in PBS buffer pH 5.

Hydrodynamic study: In order to study the electro-kinetics of electrocatalytic reduction of O_2 by the laccase-MWCNT-NA, rotating disk studies were carried out between 500 and 2000 rpm. It is know that increasing RDE rotation rates lead to a faster supply of oxygen to the electrode surface and greater turbulence near the electrode surface, which affect the oxygen diffusion to the electrode surface. For large negative overpotential applied, the cathodic response corresponds to that value limited by the maximum rate of convective-diffusional mass transport, as predicted by the so-called Levich equation for reactant species having low diffusivity (Levich, 1962):

$$i_L = 0.62nAFCD^{\frac{2}{3}}v^{-\frac{1}{6}}w^{\frac{1}{2}} = Bw^{\frac{1}{2}} \qquad (2)$$

where i_L is the limiting current, n is the number of electrons transferred per oxygen molecule, F is the Faraday constant, A is the area of the electrode, D is the diffusion coefficient, ω is the angular rotation rate, ν is the kinetic viscosity (cm^2/s), and C is the concentration of the substrate in the bulk.

Fig. 5A shows the Levich plot of limiting current versus the angular rotation rate of the RDE. The linear region, angular velocity below ~1600 rad/s corresponds to the Levich region where the reaction kinetic is faster than the rate of substrate delivery to the electrode. The nonlinear region corresponds to rotation rates too high to allow for free oxygen diffuse to the electrode surface due to turbulence caused by rotation, It happens when the rotation rates exceeds ~1600 rad/s.

In order to investigate the number of electrons (n) involved in the laccase-MWCNTs-NA catalyzed oxygen reduction, the B value in Equation (2) was substituted by the slope value obtained in Fig. 5B, and n value was calculated from the slope. The resulting number of electrons transferred per oxygen molecule was 3.85.

It is well known that Koutecky-Levich equation can be used to determine the rate constant, k_a for the electrocatalytic reaction (Kou-tecky et al., 1956). This equation for the first order reaction is:

$$i^{-\frac{1}{2}} = i_k^{-\frac{1}{2}} + i_L^{-\frac{1}{2}} = i_k^{-\frac{1}{2}} + \left(Bw^{-\frac{1}{2}}\right)^{-\frac{1}{2}} \qquad (3)$$

where i is the limiting current, i_L is the mass transfer limited current given by the Levich equation, i_k is the kinetically controlled current given by the equation (4) (Brocato et al., 2012):

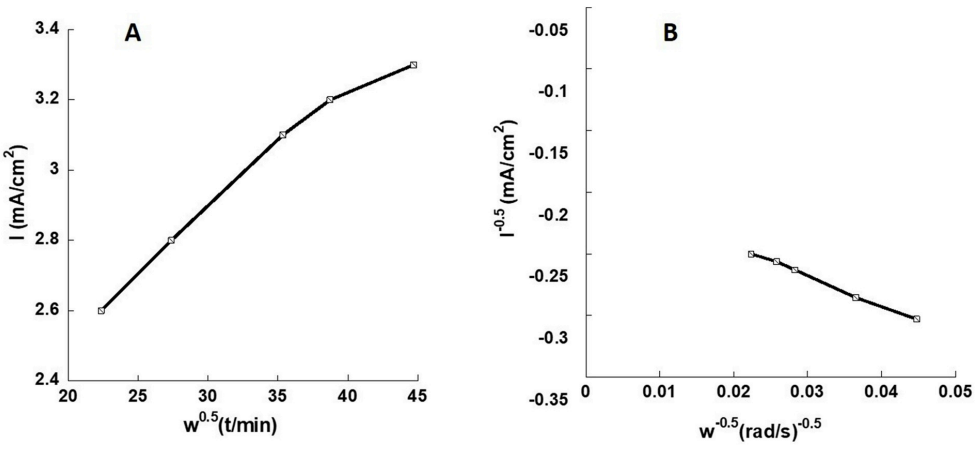

Fig. 5. (A) Levich plot of limiting current plotted against angular rotation rate of the MWCNTs-NA-Laccase modified glassy carbon electron. (B) Koutecky–Levich plot from which the kinetic constant k, (y-intercept).

$$i_k = nk_aCFD \qquad (4)$$

where k is the kinetic rate constant. The kinetic current (ik) is given by the y-intercept (1/ik) in Koutecky–Levich plot. The kinetic rate constant is calculated to be k ¼ 3 × 10^{-3} cm/s.

Recently, S. Shleev et al. (Dagys et al., 2016) developed Blue Mul-ticopper oxidases (MCO) based bioelectrocatalytic system with the T2/T3 Cu cluster connected directly to the electrode surface. The Authors demonstrated that in the case of laccase connected to the electrode surface via its T2/T3 center the redox potential is highly sensitive to the pH unlike the case where the laccase is electrically connected via T1 cluster. Moreover, the authors observes that a small concentration of F^- ions inhibited completely the electrocatalytic activity of laccases wired *via* T1 cluster unlike laccase connected via T2/T3 clusters where the electro catalytic current is still relatively high even in high concentrations of F^- (see Scheme S1). Fig. 6A shows the response of *Laccase* modified MWCNTs-NA bio-cathode at 200 mV before and after addition of 3 mM NaF solution. It can be can see that addition of NaF inhibits completely the electro-catalytic activity of laccase toward oxygen reduction. This is related toons binding to the T2/T3 cluster and preventing oxygen reduction to water.

Moreover, the response to F^- addition is very fast. It may suggest that the T2/T3 cluster is directed towards the solution as depicted in Scheme S1 A. In addition, potential values of apparition of the reduction wave at *laccase* modified MWCNTS-NA exhibits a low sensitivity to the pH of the buffer (Fig. 6B) suggesting that laccase is electrically wired *via* T1 cluster and not *via* T2/T3 cluster. Indeed, since the redox reactions involving the T1 center does not imply protons the redox potential of T1 center does not depend on pH. Thus, when laccase is wired via T1 center, the measured redox potential must be weakly affected by the variation of the solution pH. However, if the enzyme is connected to the electrode surface *via* T2/T3 cluster the redox potential should depend on the pH value because protons are involved in the reaction of electron transfer between T2/T3 center and the electrode. Analyzing the response of the system to F^- ions and to the pH changes, we can conclude that wiring the enzyme with the electrode surface involves interaction of T1 cluster of laccase with MWCNTs-NA surface.

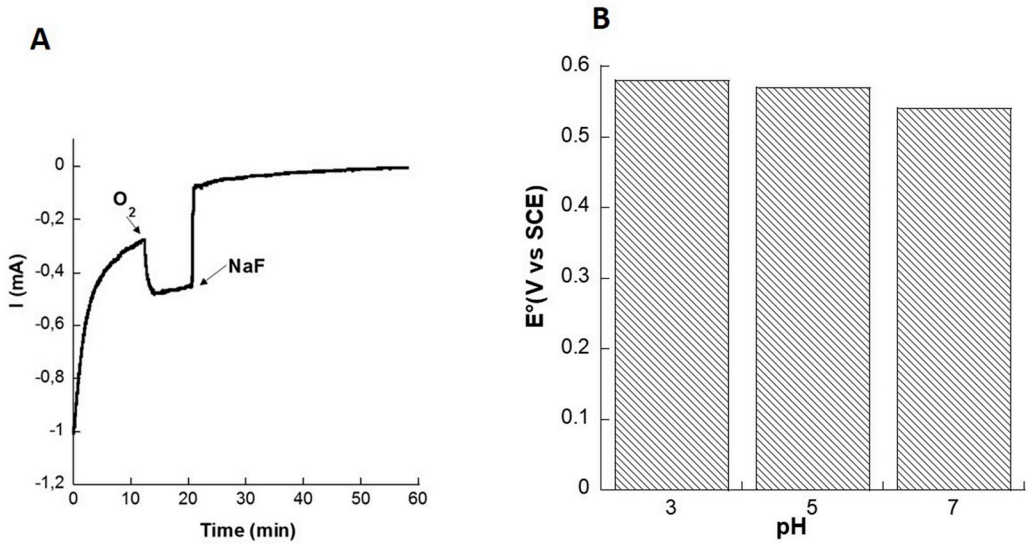

Fig. 6. (A) Chronoamperometry measurement at 200 mV of *laccase* modified MWCNTs-NA before and after saturation with oxygen, in the absence and in the presence of 3 mM NaF. (B) Potential values that correspond to the apparition of the reduction wave at *laccase* modified MWCNTs-NA at different pH values.

4. Conclusion

In this paper we report the covalent grafting of naphthalene units onto the surface of MWCNTs. Physical characterization of naphthalene modified MWCNTs shows a high level of MWCNTs functionalization. The study by QCM of the kinetics of laccase adsorption on MWCNTs-NA shows a fast laccase adsorption followed by a reorganization and conformation changes of adsorbed laccase. Our result show that elec-trical wiring of laccase does not occur directly after laccase adsorption but rather after a reorganization and conformational change of adsorbed laccase. The high density of adsorbed laccase indicates a high affinity between laccase and the surface of MWCNTs-NA, which results in a high electro catalytic activity of MWCNTs-NA-laccase surface toward oxygen reduction. We observed a direct electron transfer between the enzyme and MWCNTs-NA that exhibit a high electro-catalytic current of 3 mA cm^{-2} at potentials as high as 0.5 V *vs* SCE. A study of the electrochemical kinetics suggests that oxygen reduction involves four electrons and that the current density is not limited by the kinetics of the oxygen reduction reaction but rather by the diffusion of oxygen. We investigated the effect of pH and the presence of fluoride ions, which inhibit laccase, and our results suggest that the laccase is wired to MWCNTs-NA *via* its T1 redox center. These results indicate that functionalization of MWCNTs with naphthyl residues lead to a higher efficiency of the immobilization and favorable orientation of *Laccase*, which significantly enhances the bio-electrocatalysis of oxygen reduction.

Acknowledgements

The authors thank the following organizations for financial support: Campus France (Program Polonium 2019–2020), the French National Research Agency (BioWatts project ANR-15-CE05-0003-01, ImABic project ANR-16-CE19-0007-03), The Auvergne Rhones Alpes program "cooperation international". The project was co-financed by the Polish National Agency for Academic Exchange PPN/BIL/2018/1/00204 and National Science Centre, Poland, grant number 2016/23/D/ST5/02800. DS. grants No 033150 (JFB) from Gdansk University of Technology are kindly acknowledged.

References

Antunes, E.F., Lobo, A.O., Corat, E.J., Trava-Airoldi, V.-J., Martin, A.A., Veríssimo, C., 2006. Comparative study of first- and second-order Raman spectra of MWCNT at visible and infrared laser excitation. Carbon 44 (11), 2202–2211.

Arrocha, A.A.1, Cano-Castillo, U.2, Aguila, S.A.3, Vazquez-Duhalt, R.4, 2014. Enzyme orientation for direct electron transfer in an enzymatic fuel cell with alcohol oxidase and laccase electrode. Biosens. Bioelectron. 61, 569–574.

Bahr, Jeffrey L., Yang, Jiping, Kosynkin, Dmitry V., Bronikowski, Michael J., Smalley, Richard E., Tour, James M., 2001. Functionalization of carbon nanotubes by electrochemical reduction of aryl diazonium salts: a bucky paper electrode. J. Am. Chem. Soc. 123, 6536–6542.

Bertrand, T., Jolivalt, C., Briozzo, P., Caminade, E., Joly, N., Madzak, C., Mougin, C., 2002. Crystal structure of a four-copper laccase complexed with an arylamine: insights into substrate recognition and correlation with kinetics. Biochemistry 41, 7325–7333.

Bingen, P., Wang, G., Steinmetz, N.F., Rodahl, M., Richter, R.P., 2008. Solvation effects in the quartz crystal microbalance with dissipation monitoring response to biomolecular adsorption. A phenomenological approach. Anal. Chem. 80, 8880–8890.

Blanford, C.F., Heath, R.S., Armstrong, F.A., 2007a. A stable electrode for high-potential, electrocatalytic O2 reduction based on rational attachment of a blue copper oxidase to a graphite surface. Chem. Commun. 17, 1710–1712.

Blanford, Christopher F., Heath, Rachel S., Armstrong, Fraser A., 2007b. A stable electrode for high-potential, electrocatalytic O2 reduction based on rational attachment of a blue copper oxidase to a graphite surface. Chem. Commun. 2007, 1710–1712.

Blanford, C.F., Foster, C.E., Heath, R.S., Armstrong, F.A., 2008. Efficient electrocatalytic oxygen reduction by the "blue" copper oxidase, laccase, directly attached to chemically modified carbons. Faraday Discuss 140, 319–335.

Brocato, Shayna, Lau, Carolin, Atanassov, Plamen, 2012. Mechanistic study of direct electron transfer in bilirubin oxidase. Electrochim. Acta 61, 44–49.

Dagys, M., Laurynenas, A., Ratautas, D., Kulys, J., Vidzunaite_, R., Talaikis, M., Niaura, G., Marcinkeviciene, L., Meskysa, R., Shleev, S., 2016. Oxygen electroreduction catalysed by laccase wired to gold nanoparticles via the trinuclear copper cluster. Energy Environ. Sci. 10, 498–502, 2017.

Grobert, N., 2007. Carbon nanotubes - becoming clean. Mater. Today 10, 28–35.

Kariuki, J.K., McDermott, M.T., 1999. Nucleation and growth of functionalized aryl films on graphite electrodes. Langmuir 15, 6534–6540.

Koutecky, J., Levich, V.G., Khim, Zh Fiz, 1956. The use of rotating disk on the studies of kinetic and electrolytoc process. Zh. Fiz. Khim. 32, 1565.

Krikstolaityte, Vida, Barrantes, Alejandro, Ramanavicius, Arunas, Arnebrant, Thomas, Shleev, Sergey, Ruzgas, Tautgirdas, 2014. Bioelectrocatalytic reduction of oxygen at gold nanoparticles modified with laccase. Bioelectrochemistry 95, 1–6. Lalaoui, N., Le Goff, A., Holzinger, M., Cosnier, 2015. Fully oriented bilirubin oxidase on porphyrin-functionalized carbon nanotube electrodes for electrocatalytic oxygen reduction S. Chem. Eur J. 21, 16868–16873.

Lalaoui, N., David, R., Jamet, He, Holzinger, M., Le Goff, A., Cosnier, S., 2016. Hosting adamantane in the substrate pocket of laccase: direct bioelectrocatalytic reduction of O2 on functionalized carbon nanotubes. ACS Catal. 6, 4259–4264. Le Goff, A., Holzinger, M., Cosnier, S., 2015. Recent progress in oxygen-reducing laccase biocathodes for enzymatic biofuel cells. Cell. Mol. Life Sci. 72, 941–952.

Levich, V.G., 1962. Physicochemical Hydrodynamics, 2nd. ed. Prentice-Hall, Englewood Cliffs, N. J., pp. 60–72

Osswald, S., Havel, M., Gogotsi, Y., 2007. Monitoring oxidation of multiwalled carbon nanotubes by Raman spectroscopy. J. Raman Spectrosc. 38 (6), 728–736.

Pita, M., Shleev, S., Ruzgas, T., Ferna ndez, V.M., Yaropolov, A.I., Gorton, L., 2006. Direct heterogeneous electron transfer reactions of fungal laccases at bare and thiol modified gold electrodes. Electrochem. Commun. 8, 747–753.

Rebelo, Susana L.H., Guedes, Alexandra, Szefczyk, Monika E., Pereira, Andr e M., Araújo, Jo~ao P., Freire, Cristina, 2016. Progress in the Raman spectra analysis of covalently functionalized multiwalled carbon nanotubes: unraveling disorder in graphitic materials. Phys. Chem. Chem. Phys. 18, 12784–12796.

Sadowska, K., Jabłonowska, E., Stolarczyk, K., Wiser, R., Bilewicz, R., Roberts, K.P., Biernat, J.F., 2008. Chemically modified carbon nanotubes: synthesis and implementation. Pol. J. Chem. 82, 1309–1313.

Sadowska, K., Roberts, K.P., Wiser, R., Biernat, J.F., Jabłonowska, E., Bilewicz, R., 2009 Synthesis, characterization, and electrochemical testing of carbon nanotubes derivatized with azobenzene and anthraquinone. Carbon 47, 1501–1510.

Sajjadi, S., Ghourchian, H., Rahimi, P., 2011. Different behaviors of single and multiwall carbon nanotubes for studying electrochemistry and electrocatalysis of choline oxidase. Electrochim. Acta 56, 9542–9548.

Sauerbrey, G., 1959. Use of quartz vibration for weighing thin films on a microbalance. J. Phys. 155, 206–212.

Shleev, S., Christenson, A., Serezhenkov, V., Burbaev, D., Yaropolov, A., Gorton, L., Ruzgas, T., 2005. Electrochemical redox transformations of T1 and T2 copper sites in native Trametes hirsuta laccase at gold electrode. Biochem. J. 385, 745–754.

Solomon, E.I., Heppner, D.E., Johnston, E.M., Ginsbach, J.W., Cirera, J., Qayyum, M., Kieber-Emmons, M.T., Kjaergaard, C.H., Hadt, R.G., Tian, L., 2014. Copper active sites in biology. Chem. Rev. 114, 3659–3853.

Stolarczyk, K., Łyp, D., Z_ elechowska, K., Biernat, J.F., Rogalski, J., Bilewicz, R., 2012.Arylated carbon nanotubes for biobatteries and biofuel cells. Electrochim. Acta 79, 74–81.

Yoshida, H., 1883. Chemistry of lacquer (Urushi) part 1. J. Chem. Soc. 43, 472–486. Z_ elechowska, K., Stolarczyk, K., Łyp, D., Rogalski, J., Roberts, K.P., Bilewicz, R.,

Biernat, J.F., 2013. Coupling of laccase to electrodes in biofuel cells and biobatteries. Biocybernetics and Biomedical Engineering 33, 235–245